AIP ADVANCES **8**, 025213 (2018)

Broadband infrared reflective surfaces using doped and stacked polar dielectric layers

Mohsen Janipour[a] and Kursat Sendur[b]
Faculty of Engineering and Natural Science, Sabanci University, Istanbul 34956, Turkey

(Received 6 January 2018; accepted 6 February 2018; published online 14 February 2018)

Polar dielectrics, such as SiC, are excellent candidates for operation in extreme environments due to their excellent mechanical and thermal properties. In addition, they can achieve good IR reflection in the Reststrahlen band. However, these materials have relatively narrow spectral bandwidth for reflection, especially considering that the broadband illumination sources in extreme environments. In this study, we investigated the broadband reflection properties of polar dielectrics by engineering the Reststrahlen band through doping and stacked layers. Our results indicate that by doping polar dielectrics, spectral reflection bandwidth can be significantly broadened. In addition, we demonstrate that by stacking different polar dielectric layers, the reflection spectrum of different materials can be overlapped, and thereby, significantly broader spectrum is obtained. https://doi.org/10.1063/1.5021650

I. INTRODUCTION

Polar dielectrics, such as SiC, are excellent candidates for operation in extreme environments due to their excellent thermal stability at high temperature, corrosion resistance, and good thermal properties.[1] In addition to these properties, they exhibit attractive optical properties. Polar dielectric materials, such as SiC,[2] and GaN[3] are known to demonstrate low optical loss with negative permittivity with properties in the IR regime.[4] In addition, polar dielectrics can represent negative dielectric function in the longitudinal (LO) and transverse (TO) optical phonon frequency band, which is also known as the Reststrahlen band.[4–7] An incident wave onto a polar dielectric surface exhibits a strong reflection in the Reststrahlen band. Since the Reststrahlen band for polar dielectrics occurs in the IR regime, these materials can be used to reflect the IR radiation effects in extreme environment applications. Despite their attractive optical properties to achieve IR reflection, these materials have relatively narrow spectral bandwidth for reflection, especially considering that the sources in extreme environments are broadband. It has been shown that the Reststrahlen band of III-nitride and III-V semiconductors can be extended using hybrid modes.[8–10] In this study, we investigated the reflective properties of intrinsic and doped polar dielectrics when deposited as a single layer or double stacked layer configurations. First, we demonstrate that by doping these materials, spectral reflection bandwidth can be significantly broadened. Second, we demonstrate that by stacking different polar dielectric we managed to overlap the reflection spectrum of different materials, and thereby, significantly broaden the reflection spectrum of the composite material.

II. THEORETICAL FORMULATION

In this section, we present the theoretical method and formulations in order to achieve maximum reflection coefficient in the IR regime. First, a theoretical closed-form formulation is presented

[a]mjanipour@sabanciuniv.edu,
[b]sendur@sabanciuniv.edu.

for investigating the effect of increasing the doping concentration on the broadening the reflection spectrum at the interface of vacuum and single polar dielectric based on Fresnel reflection coefficients.[11]

Second, obtaining the maximum reflection is theoretically studied for double stacked layers consisting of SiC, and GaN; and a theoretical formulation is presented. A schematic illustration of the stacked geometries considered in this study is provided in Fig. 1(a), and 1(b), where the layers of undoped and doped polar dielectrics are stacked with their individual substrates and illuminated by a planar wave.

A. Single layer interface

Throughout this manuscript, we deal with the reflectivity properties of 4H-SiC and cubic-GaN because of their wide Reststrahlen spectral band among the polar-dielectrics.[3–5,12–14] The optical dielectric function of the polar dielectric materials (with j = SiC, and GaN) can be represented as $\varepsilon_j(\omega) = \varepsilon_{Lorentz,j}(\omega) + \varepsilon_{Drude,j}(\omega)$ with:[3,15,16]

$$\begin{aligned} \varepsilon_{Lorentz,j}(\omega) &= \varepsilon_{\infty,j}\left[1 + \frac{\omega_{LO,j}^2 - \omega_{TO,j}^2}{\omega_{TO,j}^2 - \omega(\omega + i\Gamma_j)}\right] \\ \varepsilon_{Drude,j}(\omega) &= -\frac{\omega_{p,j}^2}{\omega(\omega + i\gamma_j)}; \omega_{p,j} = \sqrt{\frac{4\pi.n.e^2}{m_j^*}} \end{aligned} \tag{1}$$

where, $\varepsilon_{\infty,j}$ is the high-frequency permittivity constant, $\omega_{LO,j}$ and $\omega_{TO,j}$ demonstrate the longitudinal, and transverse optical phonon frequencies, respectively, with considering damping frequency of Γ_j.[5,17] It should be noted that, in the theoretical and numerical simulations for GaN we considered that $\omega_{TO,GaN} \approx 16$ [THz], $\omega_{LO,GaN} \approx 22$ [THz], and $\Gamma_{GaN} \approx 0.1$ [THz]; and for SiC

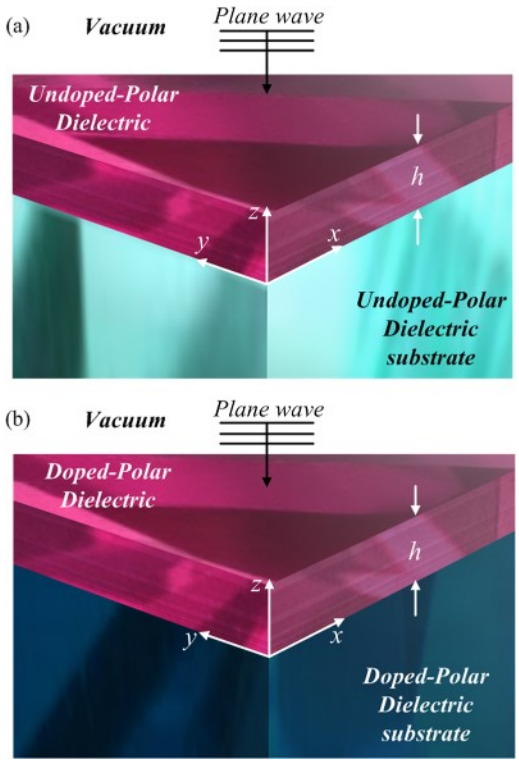

FIG. 1. Schematic representation of the stacked layers of (a) undoped polar dielectric substrate, (b) doped polar dielectric, respectively.

$\omega_{TO,SiC}\approx 24$ [THz], $\omega_{LO,SiC}\approx 29$ [THz], $\Gamma_{SiC}\approx 0.08$ [THz]. Though, the polar dielectrics are uniaxially anisotropic materials, all the parameters and calculations in this paper are based on the excitation along perpendicular axis. For materials used in this study, the surface-phonon polariton (SPhP) modes[18] and surface-plasmon (SP) modes[2,4,19] can be supported on the interfaces involving polar dielectrics with other insulator. Furthermore, since the Reststrahlen band lies in the IR frequencies, use of polar dielectrics such as SiC are attractive for extreme environment applications.[20–24] In the case of normal incidence of a plane-wave, the reflection from the interface of a polar dielectric and vacuum can be obtained by $R=|n_j-1|^2/|n_j+1|^2$ assuming $n_j=\sqrt{\varepsilon_j}$. Consequently, it can be theoretically, shown that the frequencies in which the perfect reflection may occur are as follows:

$$\omega_{\pm,j}=\sqrt{\frac{\xi_j+u_{\pm,j}\times\eta_j+\psi_{0,j}\times(u_{\pm,j}\times\eta_j)^{-1}}{-3\varepsilon_{\infty,j}}}, \tag{2}$$

where

$$\begin{pmatrix}\xi_j\\ \eta_j\\ u_{\pm,j}\\ \psi_{0,j}\\ \psi_{1,j}\\ \rho_j\\ \kappa_j\end{pmatrix}=\begin{pmatrix}\varepsilon_{\infty,j}\left(\Gamma_j^2+\gamma_j^2-\omega_{LO,j}^2-\omega_{TO,j}^2\right)-\omega_{p,j}^2\\ \left[0.5\times\left(\psi_{1,j}+\sqrt{\psi_{1,j}-4\psi_{0,j}^3}\right)\right]^{1/3}\\ 0.5\times(-1\pm i\sqrt{3})\\ \xi_j^2-3\varepsilon_{\infty,j}\times\kappa_j\\ \xi_j\left(2\xi_j^2-9\varepsilon_{\infty,j}\times\kappa_j\right)+27\varepsilon_{\infty,j}^2\times\rho_j\\ \omega_{TO,j}^2\left(\varepsilon_{\infty,j}\times\omega_{LO,j}^2\gamma_j^2-\omega_{p,j}^2\omega_{TO,j}^2\right)\\ -\varepsilon_{\infty,j}\left[\gamma_j^2\left(\omega_{LO,j}^2+\omega_{TO,j}^2-\Gamma_j^2\right)+\omega_{LO,j}^2\omega_{TO,j}^2\right]+\omega_{p,j}^2\left[2\omega_{TO,j}^2-\Gamma_j^2\right]\end{pmatrix} \tag{3}$$

Figure 2, shows $\omega_{\pm,j}$ versus doping densities in order to understand the doping effects on the broadening of the Reststrahlen band of SiC and GaN. In the case of the doped SiC, it is considered that $\gamma_{SiC}(n)=e/[m_{SiC}^*\cdot\mu_{SiC}(n)]$ with effective mass and electron mobility of $m_{SiC}^*=0.36m_0$ and $\mu_{SiC}(n)=4.82\times10^9\times n^{-0.424}\text{cm}^2\text{V}^{-1}$ while for the doped GaN; $\mu_{GaN}=440\text{cm}^2\text{V}^{-1}$ and $m_{GaN}^*=0.18m_0$ where m_0 is the electron mass.[25] It can be seen from Fig. 2 that increasing the doping density can intensively affect $\omega_{+,j}$ frequencies, while it may not affect $\omega_{-,j}$. In fact, the $\omega_{-,j}$ frequency that remains constant over the several doping concentrations represents $\omega_{TO,j}$ which is the pole of dielectric function according to Eq. (1).

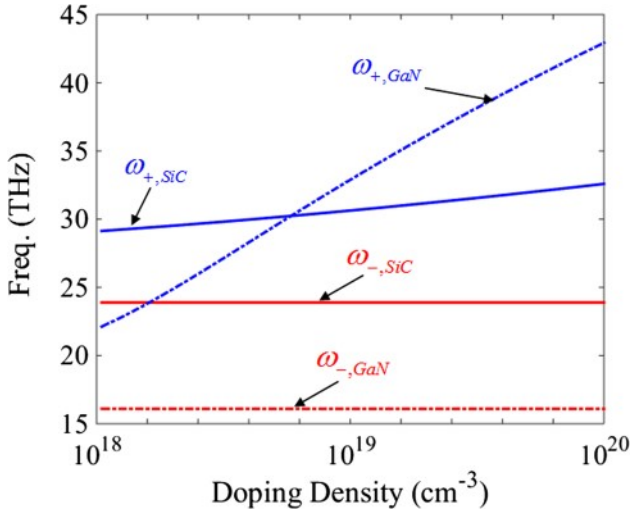

FIG. 2. The $\omega_{\pm}$ frequencies versus doping density for SiC and GaN.

Consequently, based on Fig. 2, it is obvious that the Reststrahlen band (i.e. $\omega_{+,j}$–$\omega_{-,j}$) of the doped GaN is a wider in comparison to the doped SiC. Since polar dielectrics may not yield wideband reflection, the use of heavily doped polar dielectrics is suggested as an alternative in Section IV of this manuscript.

B. Stacked layers interface

For the double stacked layers structures similar to the configuration shown in Fig. 1, it can be shown that the total reflection spectrum can be obtained by $R = \left(r_{jk} + r_{kl}e^{2i\theta_k}\right) / \left(1 + r_{jk}r_{kl}e^{2i\theta_k}\right)$ with $r_{jk} = (n_j - n_k)/(n_j + n_k)$ and $\theta_k = \omega \cdot h \cdot n_k/c$, c as the speed of light and $j \neq k \neq l$ = 1-3, respectively.[11,26,27] The theoretical formulation for the transmission and absorption spectrums regarding to the refractive indices of the structure shown in Figs. 1(a) and 1(b) can also be found in the literature.[11,26,27] However, as our investigation throughout this manuscript mainly deals with the reflection spectrum, we focus on the spectral features related to reflection spectrum. In order to study the effects of the first upper film and substrate stacked layers on the optical behavior of the stacked layers, we focus on the frequencies and conditions in which the maximum reflection can be obtained. We note that the perfect reflection may not be achieved due to the presence of the electron and phonon damping in the dielectric polar layers. One solution arises from the maximum reflection of the first layer that we discussed and theoretically obtained the frequencies in Section II, in which the maximum reflection can occur using Eq. (2) and Eq. (3). The second solution arises from $r_{kl} = e^{-2i\theta_k}$ which after some mathematical simplifications and considering the real part of the dielectric function results in; $\mathrm{Re}\left[\varepsilon_k\right]^2 - 2\left(1 + 3e^{-4i\theta_k}\right) / \left(1 - e^{-4i\theta_k}\right) \mathrm{Re}\left[\varepsilon_k \varepsilon_l\right] + \mathrm{Re}[\varepsilon_l]^2 = 0$ that can be demonstrated as:

$$\mathrm{Re}\left[\varepsilon_k\right] = -\delta_{\pm}\, \mathrm{Re}\left[\varepsilon_l\right] \tag{4}$$

where

$$\delta_{\pm} = \frac{\left(e^{-i8\theta_k} + 6e^{-i4\theta_k} + 1\right) \pm 4e^{-i2\theta_k} \cdot \left(1 + e^{-i4\theta_k}\right)}{\left(1 - e^{-i4\theta_k}\right)^2} \tag{5}$$

Thus, by using Eq. (4) and Eq. (5) and replacing in the dielectric functions of the mediums using the Drude-Lorentz classical oscillator model of Eq. (1) in Eq. (4) we obtain:

$$\begin{aligned} &\varepsilon_{\infty,k}\left[\frac{(\omega_{LO,k}^2 - \omega^2)\cdot(\omega_{TO,k}^2 - \omega^2) + \Gamma_k^2\omega^2}{(\omega_{TO,k}^2 - \omega^2)^2 + \Gamma_k^2\omega^2}\right] - \frac{\omega_{p,k}^2}{\omega^2 + \gamma_k^2} \\ &= -\delta_{\pm}\left\{\varepsilon_{\infty,l}\left[\frac{(\omega_{LO,l}^2 - \omega^2)\cdot(\omega_{TO,l}^2 - \omega^2) + \Gamma_l^2\omega^2}{(\omega_{TO,l}^2 - \omega^2)^2 + \Gamma_l^2\omega^2}\right] - \frac{\omega_{p,l}^2}{\omega^2 + \gamma_l^2}\right\} \end{aligned} \tag{6}$$

In the case of the considered materials i.e., SiC and GaN we can approximately assume that $\varepsilon_{\infty,l} \approx \varepsilon_{\infty,k}$; moreover, it can be shown that $\Gamma_l = \Gamma_k = 0$ and thus the optical phonon damping frequencies cannot impact the results. Hence, we achieve:

$$\frac{(\omega_{LO,k}^2 - \omega^2)}{(\omega_{TO,k}^2 - \omega^2)} + \delta_{\pm}\frac{(\omega_{LO,l}^2 - \omega^2)}{(\omega_{TO,l}^2 - \omega^2)} = \frac{\omega_{p,l}'^2}{\omega^2 + \gamma_l^2} + \frac{\delta_{\pm}\omega_{p,k}'^2}{\omega^2 + \gamma_k^2} \tag{7}$$

where $\omega_{p,l}'^2 = \omega_{p,l}^2/\varepsilon_{\infty,l}$ and $\omega_{p,k}'^2 = \omega_{p,k}^2/\varepsilon_{\infty,k}$. Simplifying Eq. (7) leads to an eighth-degree polynomial equation so that, its solution results in the frequencies in which the maximum reflection occurs:

$$\begin{aligned} &A_0\omega_{\pm}^8 + (A_0D_0 - B_0 - H_0)\,\omega_{\pm}^6 + (A_0E_0 - B_0D_0 + C_0 + F_0H_0 - I_0)\,\omega_{\pm}^4 \\ &+ (C_0D_0 - B_0E_0 - G_0H_0 + F_0I_0)\,\omega_{\pm}^2 + (C_0E_0 - G_0I_0) = 0 \end{aligned} \tag{8}$$

with

$$\begin{Bmatrix} A_0 \\ B_0 \\ C_0 \\ D_0 \\ E_0 \\ F_0 \\ G_0 \\ H_0 \\ I_0 \end{Bmatrix} = \begin{Bmatrix} 1+\delta_{\pm} \\ \left(\omega_{LO,k}^2+\omega_{TO,l}^2\right)+\delta_{\pm}\left(\omega_{LO,l}^2+\omega_{TO,k}^2\right) \\ \omega_{LO,k}^2\cdot\omega_{TO,l}^2+\delta_{\pm}\cdot\omega_{LO,l}^2\cdot\omega_{TO,k}^2 \\ \gamma_k^2+\gamma_l^2 \\ \gamma_k^2\cdot\gamma_l^2 \\ \omega_{TO,k}^2+\omega_{TO,l}^2 \\ \omega_{TO,k}^2\cdot\omega_{TO,l}^2 \\ \omega_{p,k}'^2+\delta_{\pm}\cdot\omega_{p,l}'^2 \\ \omega_{p,k}'^2\cdot\gamma_l^2+\delta_{\pm}\cdot\omega_{p,l}'^2\cdot\gamma_k^2 \end{Bmatrix} \tag{9}$$

According to Eq. (8) and Eqs. (9), it can be seen that although the optical phonon damping frequencies are negligible, the electron damping frequencies can strongly affect the roots of Eq. (8) and thereby the maximum reflection frequencies.

III. COMPARISON OF NUMERICAL AND THEORETICAL RESULTS

In order to confirm the theoretical results presented in the paper, the numerical solution of the considered structure is obtained. This part consists of finite-difference time-domain (FDTD) simulation method and the numerical solution of the Eq. (8) using a nonlinear equation solver.

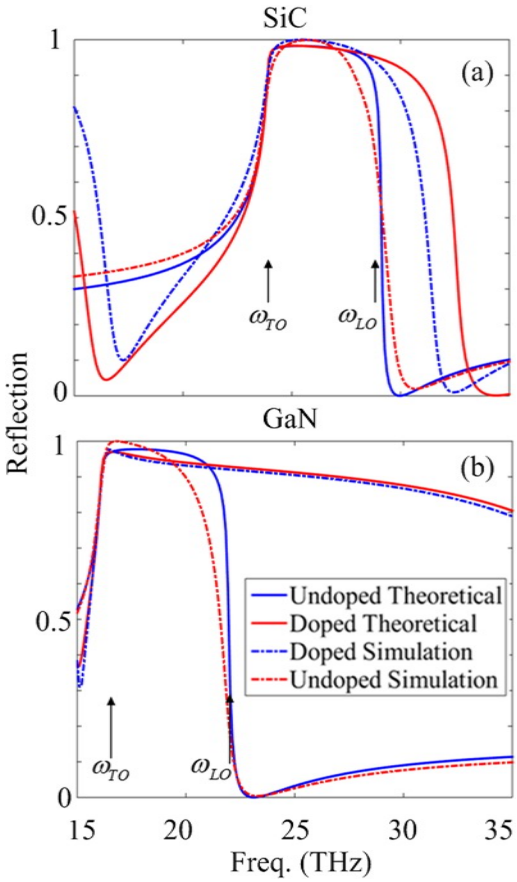

FIG. 3. The reflection spectrum obtained theoretically and numerically for the undoped and heavily-doped ($n = 10^{20}(\mathrm{cm}^{-3})$) for (a) SiC, and (b) GaN, respectively.

In the following results, a good agreement is shown between the theoretical, and the simulation results. Figures 3(a) and 3(b) demonstrate the reflection spectrum theoretically and numerically for undoped and heavily-doped ($n = 10^{20}(\text{cm}^{-3})$) SiC, and GaN, respectively. According to Figs. 3(a), and 3(b) it can be seen that ω_{TO} cannot be affected by increasing the doping density, however, ω_{LO} dramatically blue-shifts by doping which confirms the obtained theoretical results using Eq. (2) shown in Fig. 2 (i.e. $\omega_{\pm,SiC}$ and $\omega_{\pm,GaN}$). In addition, it can be seen that, increasing the doping values can reduce the reflection coefficient especially for the heavily doped GaN. Furthermore, Figs. 4(a)-4(d) demonstrate the reflection (blue solid-curve) and transmission (blue dashed-dotted-curve) obtained theoretically using Fresnel equations and the relevant simulation results of reflection (red solid-curve) and transmission (red dashed-dotted-curve) for undoped [(a), (b)], and doped ($n = 10^{20}(\text{cm}^{-3})$) layered materials [(c), (d)] for $h = 1$ and 1.5 (μm), respectively. Based on Figs. 4(a)-4(d) it can be seen that although some deviations exist between the theory and simulation, the results show a good agreement and similar trends are observed in both solutions.

Figure 5 demonstrate the theoretical reflection spectrum results for double stacked layers of lossy mediums[26] doping densities of $n = 10^{18}(\text{cm}^{-3})$ [solid-curve], $n = 10^{19}(\text{cm}^{-3})$ [dashed-curve], and $n = 10^{20}(\text{cm}^{-3})$ [dashed-dotted-curve], respectively.

In addition, Figure 5, represents the averaged summation of reflection spectrum at frequencies solved numerically using Eq. (2) and Eq. (8) $n = 10^{18}(\text{cm}^{-3})$ [circles], $n = 10^{19}$ (cm^{-3}) [diamonds], and $n = 10^{20}(\text{cm}^{-3})$ [cubes], respectively.

The results in Fig. 5 suggest that although minimum reflections occur at $\omega_{TO,SiC}$ and $\omega_{TO,GaN}$, an additional minimum in the reflection spectrum emerges between 15 THz and 20 THz due to increasing the doping density in SiC (similar to Fig. 3(a)) which is blue-shifted by adding more dopants. Furthermore, minimum reflection at higher frequencies are obvious that are due to interactions of the doped $\omega_{LO,SiC,doped}$ and $\omega_{LO,GaN,doped}$ which blue-shifts by increasing doping value. It can be noticed that in the spectral region between $\omega_{TO,SiC}$ and $\omega_{TO,GaN}$; the reflection decreases by increasing the doping while the reflection increases by doping between $\omega_{LO,SiC,doped}$ and $\omega_{LO,GaN,doped}$. Also in Fig. 5, a good agreement exists between the theoretical and numerical results.

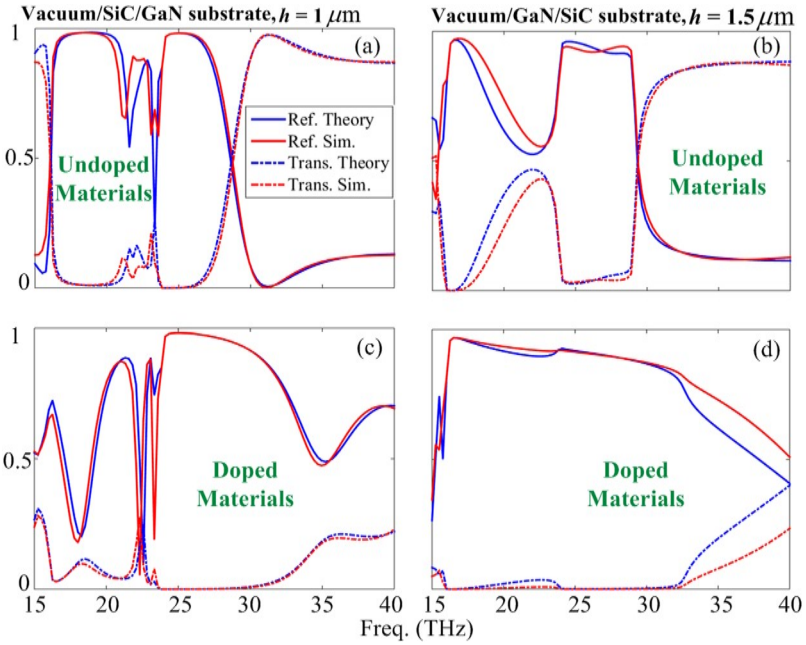

FIG. 4. The theoretically obtained reflection (blue solid-curve) and transmission (blue dashed-dotted-curve); simulation results of reflection (red solid-curve) and transmission (red dashed-dotted-curve) for undoped [(a), (b)], and heavily-doped ($n = 10^{20}(\text{cm}^{-3})$) layered materials [(c), (d)], respectively.

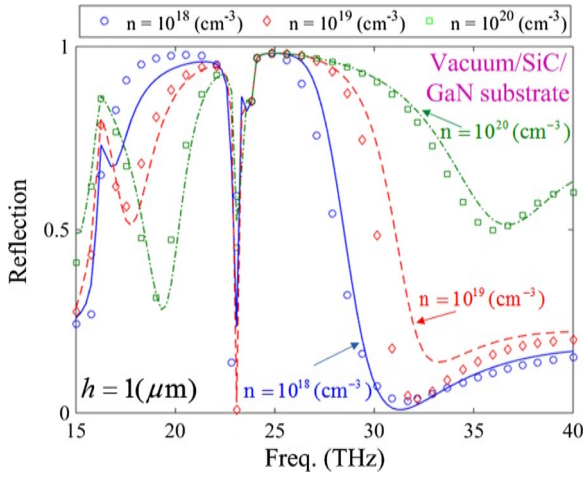

FIG. 5. The reflection spectrum theoretically obtained from Fresnel equation for $n = 10^{18}(\text{cm}^{-3})$ [solid-curve], $n = 10^{19}(\text{cm}^{-3})$ [dashed-curve], and $n = 10^{20}(\text{cm}^{-3})$ [dashed-dotted-curve]; the averaged reflection spectrum of $n = 10^{18}(\text{cm}^{-3})$ [circles], $n = 10^{19}(\text{cm}^{-3})$ [diamonds], and $n = 10^{20}(\text{cm}^{-3})$ [cubes] at frequencies obtained by numerical solution results of Eq. (2) and Eq. (8).

IV. RESULTS AND DISCUSSIONS

In this section, we present and discuss results related to spectral broadening of polar dielectrics. As we previously discussed, it is desirable to increase the spectral reflectivity over a broad spectrum to reduce the radiative load. To achieve this, we demonstrate that by doping these materials, spectral reflection bandwidth can be significantly broadened. In Figures 6(a)-6(c), and 6(d)-6(f) depict the spectral variations of reflection, transmission, and absorption coefficient of vacuum-SiC, and -GaN

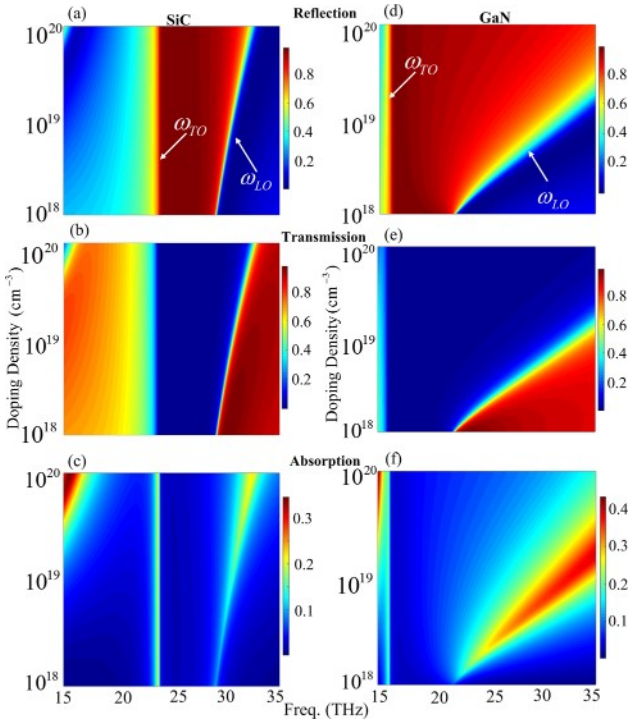

FIG. 6. Spectral variation of the reflection, transmission, and absorption coefficients versus doping density for [(a)-(c)] SiC, and [(d)-(f)] GaN of the vacuum/polar dielectric single interface.

single interface versus n-doping densities, respectively. Based on the results in Figs. 6(a), and 6(d), it is clear that increasing the doping values can drastically enhance the bandwidth of reflection spectrum of GaN in comparison to SiC. In other words, doping GaN results in wider a Reststrahlen band, however, the reflection coefficient amplitude of the doped GaN medium gradually reduced by frequency where it remains approximately constant for the doped SiC.

This can be also understood from the transmission coefficient spectrum in which the maximum transmission amplitude occurs for frequencies greater than ω_{LO} of the individual polar dielectric [Figs. 6(b), 6(e)]. Based on the results in Figs. 6(a)-6(f) the optical properties are constant around the individual ω_{TO}, the governing optical mechanism in this method is to increase the reflection bandwidth by blue-shifting the ω_{LO} frequency. Furthermore, it can be seen that the absorption coefficient increases approximately around ω_{LO} by increasing the doping density. The impact of the doping densities on the ω_{LO} in this method of widening of the reflection coefficient bandwidth plays the most important role.

To improve the reflectivity of the presented doped polar dielectrics, one can utilize the stacked layers structure of polar dielectrics. Another major parameter in this kind of applications is the thickness of the polar dielectric medium. In the next set of results we investigate the effect of thickness in the undoped and doped SiC/GaN stacked layers which can effectively reflect the IR radiations. Figures 7(a1)-7(c1), and 7(a2)-7(c2) depict the spectral variations of reflection, transmission, and absorption coefficients of vacuum/undoped SiC/undoped GaN substrate and vacuum/doped SiC/doped GaN substrate, respectively. We have considered the heavy n-doping concentration with similar density of $n = 10^{20}$ (cm^{-3}) for both of SiC and GaN mediums. Figures 8[(a1)-(c1)] and 8[(a2)-(c2)] show the spectral variations of the reflection, transmission, and absorption coefficients for the vacuum/undoped GaN/undoped SiC, and vacuum/doped GaN/doped SiC, respectively, versus the thickness of the thin layer.

According to Figs. 8[(a1)-(c1)] it can be seen that, for the thin undoped GaN layer stacked to the undoped SiC substrate, the maximum reflection gap occurs between $\omega_{LO,GaN}$ and $\omega_{TO,SiC}$.

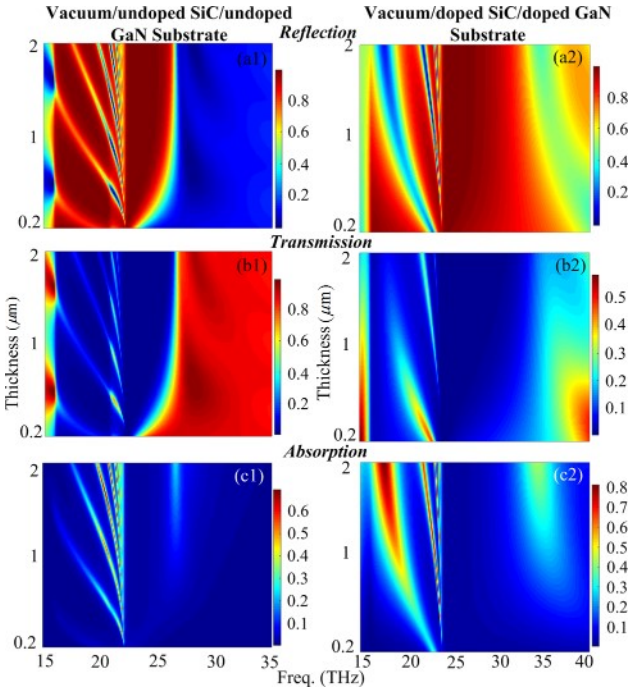

FIG. 7. Spectral variation of the reflection, transmission, and absorption coefficients versus thickness of the [(a1)-(c1)] vacuum/undoped SiC/undoped GaN substrate and [(a2)-(c2)] vacuum/doped SiC/doped GaN substrate stacked layers structure, respectively.

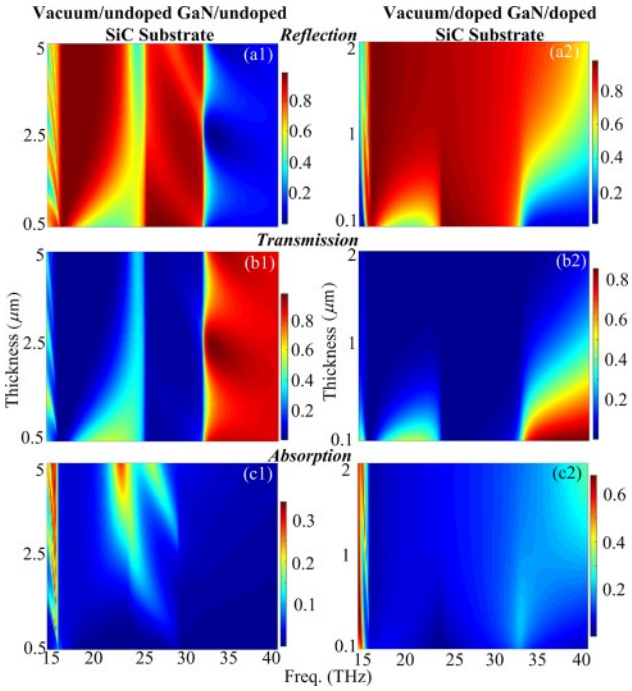

FIG. 8. Spectral variation of the reflection, transmission, and absorption coefficients versus thickness of the [(a1)-(c1)] vacuum/undoped GaN/undoped SiC substrate and [(a2)-(c2)] vacuum/doped GaN/doped SiC substrate stacked layers structure, respectively.

It is obvious that, though the GaN layer is able to absorb more radiations around 5 (μm), for the thicknesses less than 1 (μm) this frequency gap can effectively transmit the IR radiations. Furthermore, the transmission is so high for the frequencies more than $\omega_{LO,SiC}$. On the other hands, in comparison to Figs. 8[(a1)-(c1)] with Figs. 7[(a1)-(c1)], except small gaps; the undoped SiC/undoped GaN stacked layers represent continuous reflection for the lower frequencies. Besides, based on Figs. 8[(a2)-(c2)], it can be seen that increasing the thickness of the doped GaN layer can obtain continuous and wide reflection coefficient through minimizing the transmission coefficient spectrum. In fact, the latter effect is happened because the high Reststrahlen band of the doped GaN can cover the Reststrahlen band of the doped SiC substrate via enhancing the thickness. Comparing with the Figs. 7[(a2)-(c2)] one can interestingly find out that instead of using a doped GaN with several microns of thickness, a thin layer of doped SiC ($\approx$ 200 nm) deposited on a doped GaN substrate can provide a broadband reflection spectrum.

V. CONCLUSION

In conclusion, in this paper we investigate the single layer and stacked polar dielectrics with vacuum interface for potential applications in extreme environments as IR wideband reflectors. We demonstrated that broadband reflection can be obtained through engineering the Reststrahlen band of the polar dielectric mediums. Our results indicated that at the vacuum/polar dielectric interface, broadband reflection can be achieved by dramatically blue-shifting the individual ω_{LO} frequency through doping the polar dielectric. For the stacked structure, increasing the doping value results in two valleys in the reflection spectrum, where the first (lower frequency) dip blue-shifts and increases by doping. The second (higher frequency) valley decreases and blue-shifts by adding more dopants. In addition, we show that using a thin layer of doped SiC (thickness of around 200 nm) stacked on a doped GaN substrate one can achieve a discrete wide band reflection, while a doped layer of GaN (with thickness of 2 μm) is needed to be stacked on the doped SiC substrate for obtaining a reasonable continuous wideband reflection. Considering that the GaN is an expensive material, in

some cases researchers may prefer to use the separated broadband reflection of the doped layer of SiC/GaN substrate configuration.

ACKNOWLEDGMENTS

This material is based upon work supported by the Air Force Office of Scientific Research under award number FA9550-17-1-0092.

[1] C.-M. Zetterling, A. Hallén, R. Hedayati, S. Kargarrazi, L. Lanni, B. G. Malm, S. Mardani, H. Norström, A. Rusu, S. S. Suvanam, Y. Tian, and M. Östling, "Bipolar integrated circuits in SiC for extreme environment operation," Semicond. Sci. Technol. **32**, 34002 (2017).
[2] S. Law, L. Yu, A. Rosenberg, and D. Wasserman, "All-semiconductor plasmonic nanoantennas for infrared sensing," Nano Lett. **13**, 4569–4574 (2013).
[3] A. Kasic, M. Schubert, S. Einfeldt, D. Hommel, and T. E. Tiwald, "Free-carrier and phonon properties of n - and p -type hexagonal GaN films measured by infrared ellipsometry," Phys. Rev. B **62**, 7365–7377 (2000).
[4] J. D. Caldwell, L. Lindsay, V. Giannini, I. Vurgaftman, T. L. Reinecke, S. A. Maier, and O. J. Glembocki, "Low-loss, infrared and terahertz nanophotonics using surface phonon polaritons," Nanophotonics (2014).
[5] P. Y. Yu and M. Cardona, *Fundamentals of Semiconductors, Physics and Materials Properties*, 3rd ed. (Springer, 2005).
[6] J. D. Caldwell, A. V. Kretinin, Y. Chen, V. Giannini, M. M. Fogler, Y. Francescato, C. T. Ellis, J. G. Tischler, C. R. Woods, A. J. Giles, M. Hong, K. Watanabe, T. Taniguchi, S. A. Maier, and K. S. Novoselov, "Natural hyperbolic material hexagonal boron nitride," Nat. Commun. **5**, 1–9 (2014).
[7] S. Adachi, "The Reststrahlen region," in *Optical Properties of Crystalline and Amorphous Semiconductors* (Springer US, 1999), pp. 33–62.
[8] W. H. Streyer, "Reststrahlen band optics for the advancement of far-infrared optical architecture," University of Illinois at Urbana-Champaign (2016).
[9] W. Streyer, K. Feng, A. J. Hoffman, and D. Wasserman, "Engineering the Reststrahlen band with hybrid plasmon/phonon excitations," MRS Comm. **6**, 1–8 (2016).
[10] K. Feng, W. Streyer, S. M. Islam, J. Verma, D. Jena, D. Wasserman, and A. J. Hoffman, "Localized surface phonon polariton resonances in polar gallium nitride," Appl. Phys. Lett. **107**, 81108 (2015).
[11] S. J. Orfanidis, *Electromagnetic Waves and Antennas Electromagnetic Waves and Antennas* (Rutgers University, 2004).
[12] P. Li, M. Lewin, A. V. Kretinin, J. D. Caldwell, K. S. Novoselov, T. Taniguchi, K. Watanabe, F. Gaussmann, and T. Taubner, "Hyperbolic phonon-polaritons in boron nitride for near-field optical imaging and focusing," Nat. Commun. **6**, 7507 (2015).
[13] M. Kazan, S. Pereira, M. R. Correia, and P. Masri, "Directional dependence of AlN intrinsic complex dielectric function, optical phonon lifetimes, and decay channels measured by polarized infrared reflectivity," J. Appl. Phys. **106**, 23523 (2009).
[14] M. Schubert, T. E. Tiwald, and C. M. Herzinger, "Infrared dielectric anisotropy and phonon modes of sapphire," Phys. Rev. B **61**, 8187–8201 (2000).
[15] F. Demangeot, J. Frandon, M. A. Renucci, C. Meny, O. Briot, and R. L. Aulombard, "Interplay of electrons and phonons in heavily doped GaN epilayers," J. Appl. Phys. **82**, 1305–1309 (1997).
[16] T. Tiwald, J. Woollam, S. Zollner, J. Christiansen, R. Gregory, T. Wetteroth, S. Wilson, and A. Powell, "Carrier concentration and lattice absorption in bulk and epitaxial silicon carbide determined using infrared ellipsometry," Phys. Rev. B **60**, 11464–11474 (1999).
[17] H. Kuzmany, *Solid State Spectroscopy, an Introduction*, 2nd ed. (Springer, 2009).
[18] M. Janipour, I. B. Misirlioglu, and K. Sendur, "Tunable surface plasmon and phonon polariton interactions for moderately doped semiconductor surfaces," Sci. Rep. **6**, 34071 (2016).
[19] J. D. Caldwell, O. J. Glembocki, Y. Francescato, N. Sharac, V. Giannini, F. J. Bezares, J. P. Long, J. C. Owrutsky, I. Vurgaftman, J. G. Tischler, V. D. Wheeler, N. D. Bassim, L. M. Shirey, R. Kasica, and S. A. Maier, "Low-loss, extreme sub-diffraction photon confinement via silicon carbide localized surface phonon polariton resonators," Nano Lett. **13**, 3690–3697 (2013).
[20] S. Kumar, K. C. Shekar, B. Jana, L. M. Manocha, and N. Eswara Prasad, *Aerospace Materials and Material Technologies* (Springer, 2017).
[21] J. W. Zimmermann, G. E. Hilmas, W. G. Fahrenholtz, R. B. Dinwiddie, W. D. Porter, and H. Wang, "Thermophysical properties of ZrB_2 and ZrB_2 –SiC ceramics," J. Am. Ceram. Soc. **91**, 1405–1411 (2008).
[22] C. Yan, W. Lifeng, and R. Jianyue, "Multi-functional SiC/Al composites for aerospace applications," Chinese J. Aeronaut. **21**, 578–584 (2008).
[23] N. Eswara Prasad, A. Kumar, and J. Subramanyam, "Ceramic matrix composites (CMCs) for aerospace applications," in *Aerospace Materials and Material Technologies* (2017), pp. 371–389.
[24] F. Monteverde and L. Scatteia, "Resistance to thermal shock and to oxidation of metal diborides-SiC ceramics for aerospace application," J. Am. Ceram. Soc. **90**, 1130–1138 (2007).
[25] "NSM archive - optical properties," http://www.ioffe.ru/SVA/NSM/Semicond.html.
[26] W. N. Hansen, "Electric fields produced by the propagation of plane coherent electromagnetic radiation in a stratified medium," J. Opt. Soc. Am. **58**, 380 (1968).
[27] B. E. A. Saleh and M. C. Teich, *Fundamentals of Photonics* (Wiley-Interscience, 2007).